

RESEARCH ARTICLE

Transient simulation of electrochemical machining processes for manufacturing of surface structures in high-strength materials

Sascha Loebel* | Mike Zinecker | Philipp Steinert | Andreas Schubert

Professorship Micromanufacturing
Technology, Chemnitz University of
Technology, Reichenhainer Straße 70, 09126
Chemnitz, Germany

Correspondence

*Sascha Loebel, Professorship
Micromanufacturing Technology, Chemnitz
University of Technology, 09126 Chemnitz,
Germany.
Email: sascha.loebel@mb.tu-chemnitz.de

Summary

Electrochemical machining (ECM) is a method for removing metal by anodic dissolution. At the interface between the workpiece surface and an electrically conductive fluid (electrolyte), the material is dissolved locally without direct physical contact to the cathodic tool. Due to the force-free nature of the process, ECM is used for machining high-strength or hard materials, such as titanium aluminides, Inconel, Waspaloy, and high nickel, cobalt, and rhenium alloys.¹ However, determining suitable process parameters remains challenging due to their interacting effects on working distances during the machining process. Therefore a simulation-based approach to process design substantially reduces resource and time investment to achieve the desired geometry of the finished part. This methodology requires data about the materials electrochemical properties, such as removal velocity and current efficiency, which have to be obtained experimentally. In this study, a methodology for acquiring and processing this data as well as the development of multiphysics simulation models is presented for two use cases: (i) manufacturing a centrifugal impeller with a diameter of 14 mm consisting of the nickel alloy Inconel 713C for use in turbomachinery and (ii) the generation of a defined surface micro structure into the novel Mg-Y-Zn alloy WZ73.

KEYWORDS:

electrochemical machining (ECM), multiphysics simulation, process design, high-strength materials, precision manufacturing

1 | INTRODUCTION

Within the collaborative research project AMARETO of Technische Universität Bergakademie Freiberg, Dresden University of Technology, Chemnitz University of Technology and the Fraunhofer Institute for Machine Tools and Forming Technology, the higher-level objective pursued is the development of methods and transfer of solutions for parts of the value chain, focusing on time- and resource-efficiency in product development. One suitable approach is the implementation of the concept of a digital twin, a virtual representation of a physical product. This digital twin contains all available data regarding material, treatment conditions, geometry, and surface characteristics along the process chain. As this digital twin is subject to simulated process steps, this data must contain relevant input data to be integrated in simulation models via suitable interfaces.

In electrochemical machining (ECM), electrodynamic, fluid dynamic, and thermodynamic mechanisms as well as reaction kinetics are interacting with each other, influencing local electrolyte conductivity, material transport, and resulting workpiece

geometry. Consequently, achieving the desired workpiece geometry and surface properties requires multiple iterations for optimizing process configuration and tool design. Multiphysics simulation is an essential tool in order to design ECM processes efficiently.² These process simulation models rely on accurate input of the electrochemical properties of the materials to be machined, such as their normal removal velocity, current efficiency and overpotentials as functions of the normal current density. These functions are calculated from process data recorded during material characterization experiments and are subsequently integrated into process simulation models in a streamlined data processing chain. In this study, two distinct variations of ECM processes are discussed exemplarily.

The first example involves the manufacturing of a centrifugal impeller consisting of Inconel 713C for application in turbomachinery. Inconel 713C is a nickel-based superalloy featuring tensile and yield strengths above 700 MPa at temperatures up to 800 °C.³ Due to its mechanical properties conventional machining of this alloy is challenging, resulting in high tool wear, long manufacturing times, and need for additional surface finish. Alternatively, a pulsed electrochemical machining (PECM) process can be applied. In PECM, the cathode is moved into the workpiece utilizing pulsed electric current and dedicated flushing periods during pulse-off times instead of continuous current and flushing. To further improve the flushing conditions, the linear movement of the tool cathode is superimposed by an oscillation movement. Figure 1 shows the principle of pulsed electrochemical machining with oscillating cathode schematically.

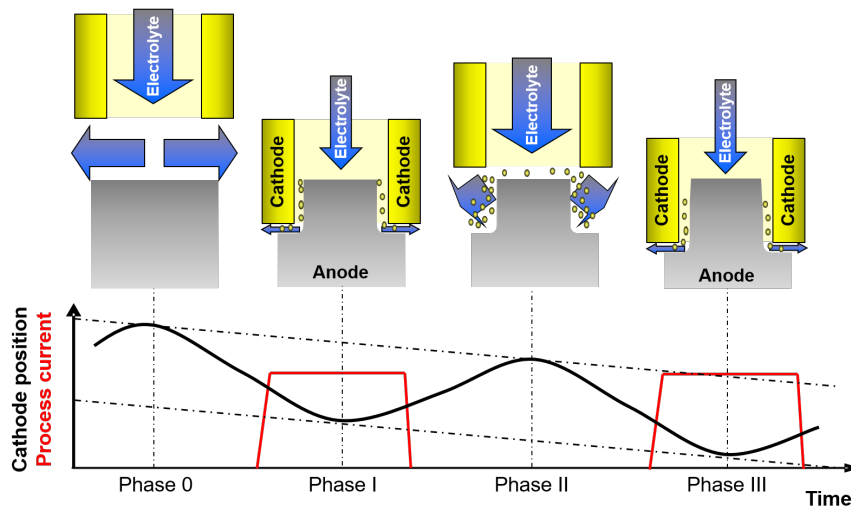


FIGURE 1 Principle of pulsed electrochemical machining (PECM) with oscillating cathode.⁴

During PECM with an oscillating cathode, working distances during pulse-on times (phase I and phase III) are minimal while the electrolyte is reliably renewed during pulse-off times (phase II), hence increasing accuracy and stability of the process.⁵ Current and oscillation frequencies typically range from 50 Hz to 200 Hz with pulse-on times of 1 ms to 4 ms.

The second example in this paper is the generation of a functional surface structure into the Mg-Y-Zn alloy WZ73. This light metal alloy provides high yield strength for temperatures up to 200 °C, thus meeting requirements prevalent in automotive and aviation engineering.⁶ Lubrication pockets in the form of micro calottes are manufactured via ECM with continuous electrolytic free jet (Jet-ECM). The principle is illustrated schematically in figure 2. In Jet-ECM, the electrolyte is focused through a cathodically connected nozzle (yellow) onto the anodically connected workpiece (grey). In this setup, the electric current is constrained to the electrolyte jet, thus resulting in high local current densities at the workpiece surface beneath. This allows for continuous highly localized material removal in an area slightly bigger than the cross section of the nozzle and assures a sufficient supply of clean electrolyte. Typically, nozzles have diameters ranging from 50 µm to 500 µm and are positioned 100 µm to 500 µm above the workpiece surface. Rate and location of material removal are adjusted by working voltage and nozzle position. Therefore, the Jet-ECM process is more flexible than sinking methods relying on a specific cathode shape.

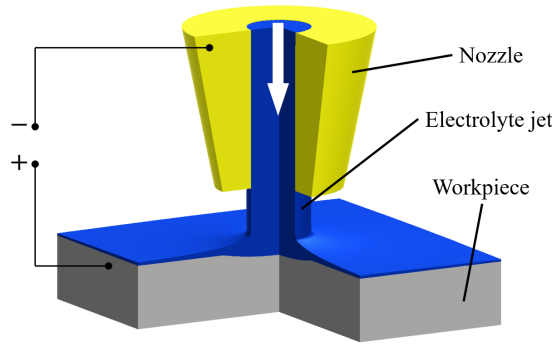


FIGURE 2 Principle of electrochemical machining with continuous electrolyte free jet (Jet-ECM).⁷

2 | SIMULATION-BASED PROCESS DESIGN

Figure 3 illustrates the developed methodology of simulation-based design of ECM processes utilizing the concept of the digital twin. At the beginning, relevant data regarding material, geometry or treatment condition of the initial or semi-finished part are extracted from the data chain of the digital twin. In combination with the requirements of the part, such as geometric tolerances or surface quality, a removal concept can be outlined. This includes the choice of a suitable machining process and its approximate input parameter intervals. If the electrochemical properties of the material are yet unknown, a removal characterization can provide all necessary information. After integrating these properties in developed models for process simulation, machining parameters can be derived. Finally, geometry and surface properties of the manufactured part can be analyzed and the information returned to the data chain of the digital twin for subsequent manufacturing steps. In this work, removal characterization and process simulation will be discussed more in-depth.

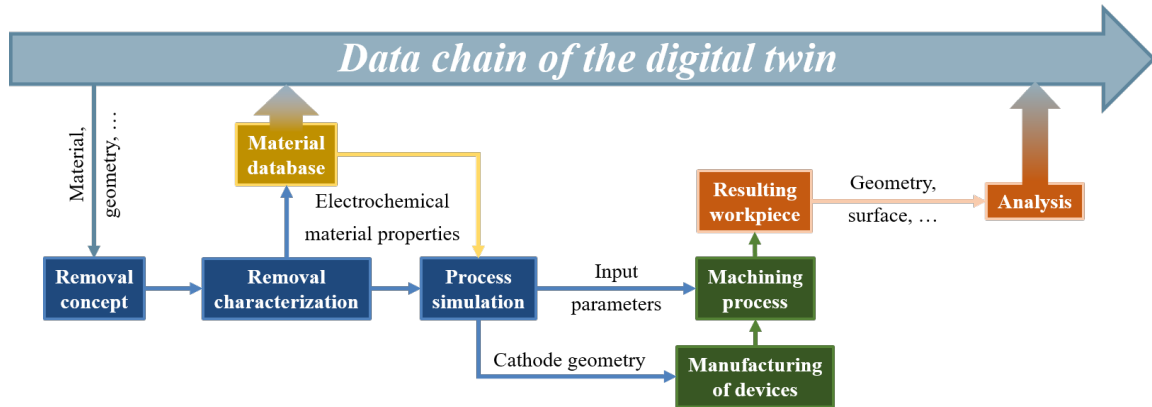


FIGURE 3 Methodology for the simulation-based design of ECM processes.

2.1 | Removal characterization

An essential material property for the development of a process simulation model is either normal removal velocity v_a , effective material removal rate V_{eff} , or current efficiency η as a function of the normal current density J , respectively. The following equation describes the relation of these quantities:⁸

$$\frac{v_a}{J} = V_{\text{eff}} = \eta V_{\text{sp}}. \quad (1)$$

V_{sp} , the specific material removal rate, can be calculated according to Faraday's law of electrolysis for an alloy of mass density ρ consisting of components indexed i with specific weights w_i , molar masses M_i and valences z_i :⁹

$$V_{sp} = (\rho F)^{-1} \sum_i \frac{w_i M_i}{z_i}. \quad (2)$$

The compositions of the characterized alloys Inconel 713C and WZ73 are shown in table 1 and table 2, respectively.

TABLE 1 Composition of Inconel 713C.

i	Ni	Cr	Mo	Nb	Ti	Fe	C	Others
w_i (%)	Bal.	13.1	6.3	4.4	2.1	0.9	0.15	< 0.28

TABLE 2 Composition of WZ73.

i	Mg	Y	Zn	Zr	Others
w_i (%)	Bal.	6.8	2.5	0.4	< 0.01

In this study, the removal characterization was conducted according to DIN SPEC 91399¹⁰, which yields the normal removal velocity v_a as a function of normal current density J at the workpiece surface as well as the sum of all overpotentials U_Σ . The latter describes the voltage drop in the boundary layers between electrodes and bulk electrolyte. U_Σ can constitute a significant percentage of the total working voltage U_q , reducing the amount of material removed electrochemically, hence it is another necessary input quantity for ECM process simulation models.

The removal characterization consists of several PECM experiments under variation of working voltage U_q and feed velocity v_f . All experiments were conducted on the manufacturing machine PEMCenter 8000 using a solution of NaNO_3 with a salt content of 8 % as electrolyte. Figure 4 displays a basic scheme of the setup. Both the cathodic tool electrode (yellow) and the anodic sample workpiece (grey) were of cylindrical shape with a diameter of 12 mm, aligned coaxially. Relevant parameters of the characterization experiments are summarized in table 3.

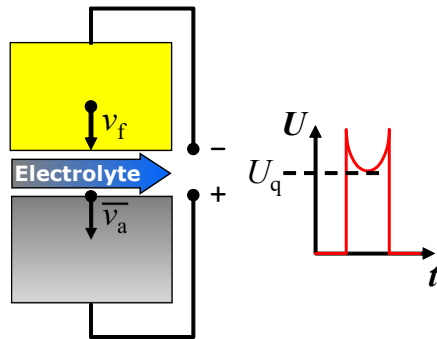


FIGURE 4 Scheme of material characterization setup. Feed velocity v_f and average removal velocity \bar{v}_a are of same magnitude and direction.

TABLE 3 Parameters of the characterization experiments.

Parameter	Characterized material	
	Inconel 713C	WZ73
Electrolyte conductivity σ_{el}	69 mS cm ⁻¹	
Electrolyte inlet pressure p_{in}	310 kPa	
Maximum feed velocity v_f	0.51 mm min ⁻¹	1.04 mm min ⁻¹
Oscillation frequency f_z	50 Hz	
Working voltage U_q	(5.0 ... 14.5) V	
Pulse frequency f_p	50 Hz	
Pulse duration t_p	4 ms	

Within the removal characterization of both materials, a total of 81 experiments were conducted while recording available process data, such as cathode position and current characteristic. Calculated removal velocities v_a and sums of overpotentials U_Σ as functions of current density J are shown in figure 5. For both alloys v_a and J are in linear relation. As these functions cross the origin of coordinates, according to equation (1) constant effective material removal rates V_{eff} of $43 \times 10^{-3} \text{ mm}^3 \text{ C}^{-1}$ and $95 \times 10^{-3} \text{ mm}^3 \text{ C}^{-1}$ at current efficiencies η of 1.36 and 1.21 can be determined for Inconel 713C and WZ73, respectively. Sums of overpotentials U_Σ ranging from 3 V to 14 V were observed.

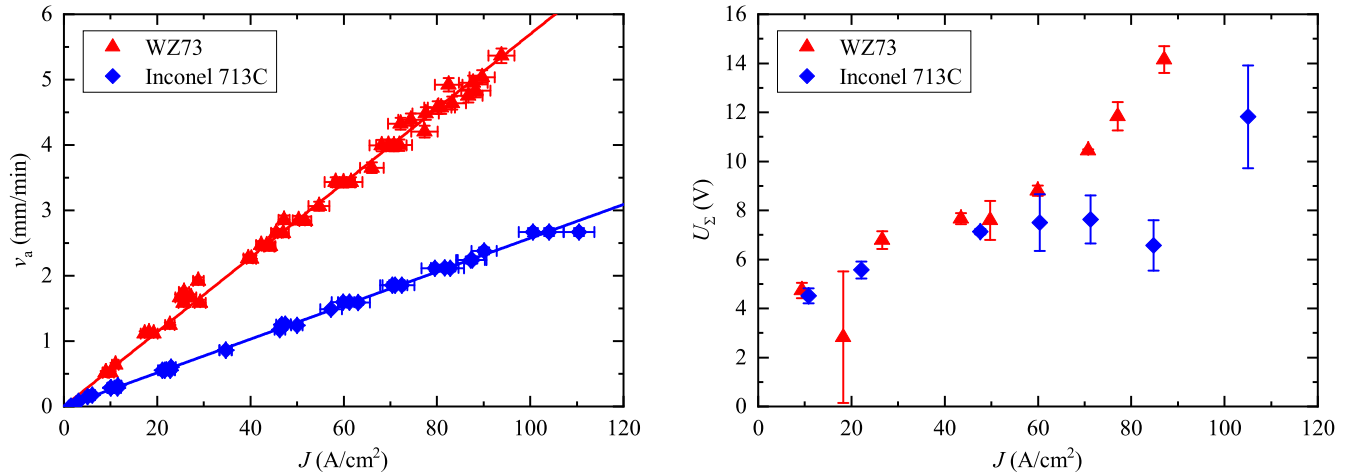


FIGURE 5 Electrochemical properties of Inconel 713C and WZ73 obtained from material characterization experiments. Normal removal velocities v_a (left) and sums of overpotentials U_Σ (right) as functions of normal current density J at the workpiece surface.

2.2 | Data processing and database integration

To perform the calculation of electrochemical properties for each material efficiently from the accumulated process data, an automated data evaluation flow as an interface between characterization experiments, a material database and the simulation environment was developed in the data science tool KNIME Analytics Platform¹¹. As outlined in the dataflow in figure 6, the result of the processed data can be displayed tabularly and graphically. After inspection, all data regarding both machined material and electrolyte properties during the material characterization experiments is reformatted and integrated into a PostgreSQL database structure set up for this purpose. This dataflow also allows accessing all data in a format suitable for integration in multiphysics simulation. As this data is available online, it can also be accessed via web interface.

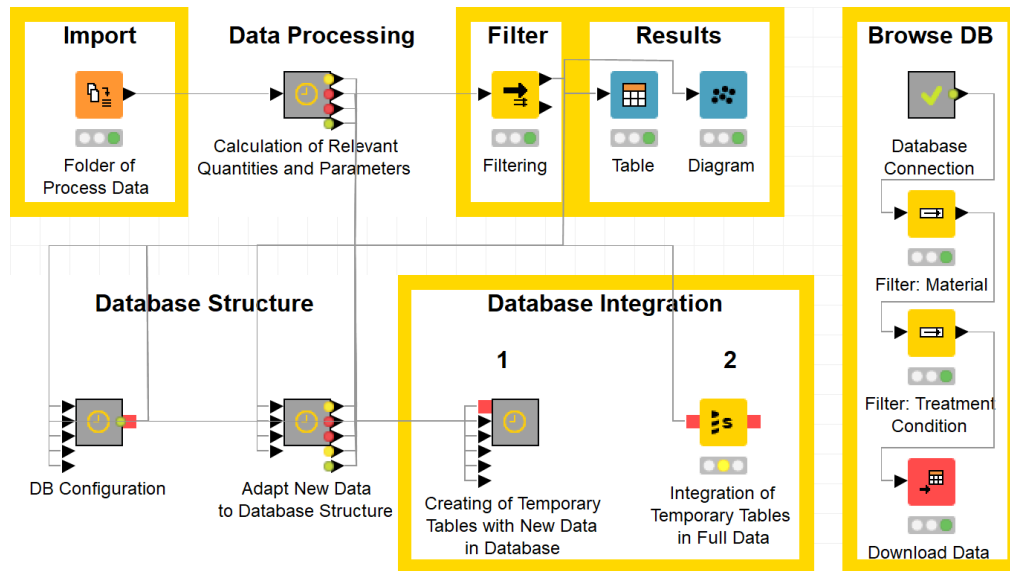


FIGURE 6 Dataflow developed in KNIME Analytics Platform for calculation of electrochemical properties from characterization experiments, interfacing to an online material database.

3 | MULTIPHYSICS SIMULATION

In this section, developed process simulation models for both the manufacturing of a centrifugal impeller consisting Inconel 713C via PECM¹² and the generation of a micro calottes in a WZ73 surface via Jet-ECM¹³ will be presented and results will be discussed briefly. Removal velocities v_a and sums of overpotentials U_Σ determined during the material characterization can be integrated into the models directly from the recorded process data or from the material database.

3.1 | Manufacturing of a centrifugal impeller via PECM

3.1.1 | Concept and methods

A 3D model of the PECM process was developed using the commercial software COMSOL Multiphysics, which utilizes the finite element method (FEM). The impeller is manufactured by moving a cathode sheet with cutouts into a cylindrical rod with a diameter of 14 mm. Utilizing the periodic shape of the impeller, the removal process was modelled only for a single segment. The basic concept is illustrated in figure 7. Based on the results of the removal characterization, promising process parameters were selected and are summarized in table 4. In order to improve the reproduction accuracy of the designed blade profile, the cathode features an isolation on top and a 45° chamfer.

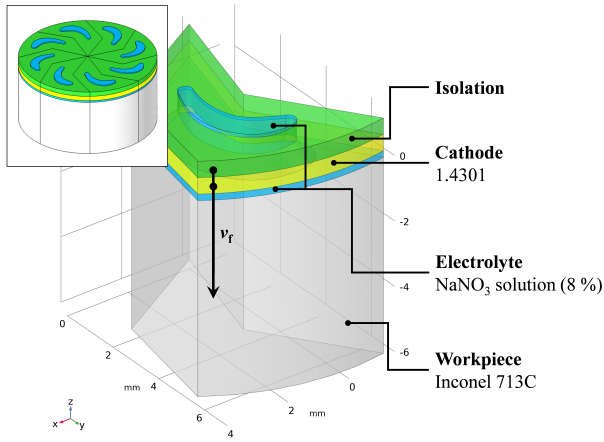


FIGURE 7 Simulation model of the PECM process for manufacturing centrifugal impellers from a cylindrical workpiece.

TABLE 4 Definition of process parameters used in the model of the PECM process.

Parameter	Value
Electrolyte conductivity σ_{el}	69 mS cm ⁻¹
Feed velocity v_f	0.5 mm min ⁻¹
Oscillation frequency f_z	50 Hz
Working voltage U_q	14.5 V
Pulse frequency f_p	50 Hz
Pulse duration t_p	4 ms
Initial working distance s_0	200 μ m
Process time t_{proc}	180 s

After defining the working voltage as a boundary condition at the cathode boundary, charge transport and resulting current densities in the electrolyte domain are determined by a potential model. This model is based on Ohm's law and the conservation of electric charge. By fully coupling electrodynamics and boundaries displacement of the workpiece domain according to the functions shown in figure 5, the material removal is calculated.

3.1.2 | Results

Figure 8 displays the simulated distribution of normal current density on the workpiece surface after a machining time of 180 s. At this point in time, the cathode has fully passed the top of the workpiece resulting in close to zero current density at this part of the workpiece, and hence no material removal. For process parameters defined in table 4, the frontal working distance converges to 46 μ m at current densities of 96 A cm⁻². At the 45° chamfer of the cathode, the increased working distance of 81 μ m decreases the current density to 68 A cm⁻². The lateral profile of the simulated impeller blade superimposed with the blade-shaped recess in the cathode is shown in figure 9. Areas of the impeller blade with concave curvature show a smaller lateral working distance with a minimum of $d_{min} = 74 \mu$ m, whereas areas of convex curvature, experiencing high current densities show distances up

to $d_{\max} = 108 \mu\text{m}$. These variation have to be accounted for in cathode design in order to obtain the desired impeller blade geometry.

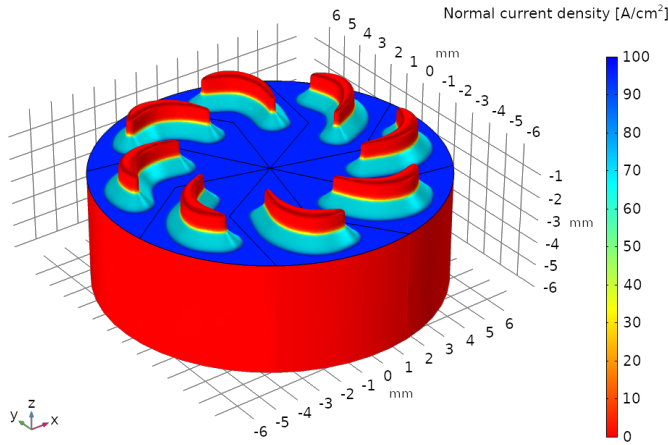


FIGURE 8 Removal geometry and normal current density distribution on the workpiece after a machining time of 180 s.

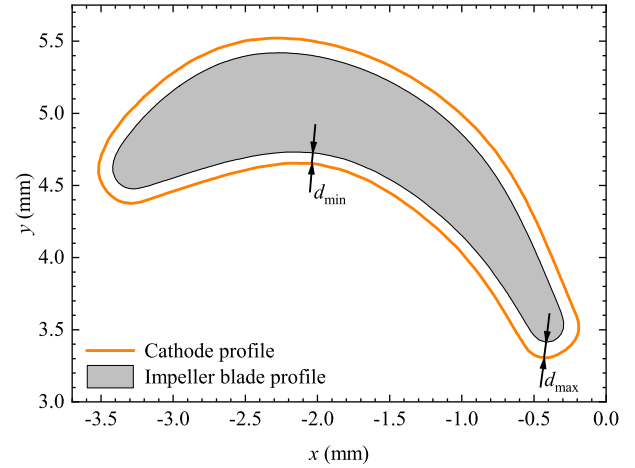


FIGURE 9 Superimposed lateral profiles of machined impeller blade (grey) and cathode (orange).

3.2 | Generation of micro calottes in WZ73 surfaces

3.2.1 | Concept and methods

In Jet-ECM process simulations not only the local electric conductivity but also the shape of the electrolyte domain heavily depend on accurate modelling of fluid dynamic conditions. In computational fluid dynamics, the finite volume method (FVM) is often preferred due to its property of exactly conserving fluxes in each finite volume. Thus the FVM simulation software Star-CCM+ was used to develop a 3D model of a Jet-ECM process for the generation of micro calottes in a WZ73 surface using a nozzle with a diameter of $100 \mu\text{m}$. The removal concept is shown in figure 10 and relevant process and material parameters are summarized in table 5.

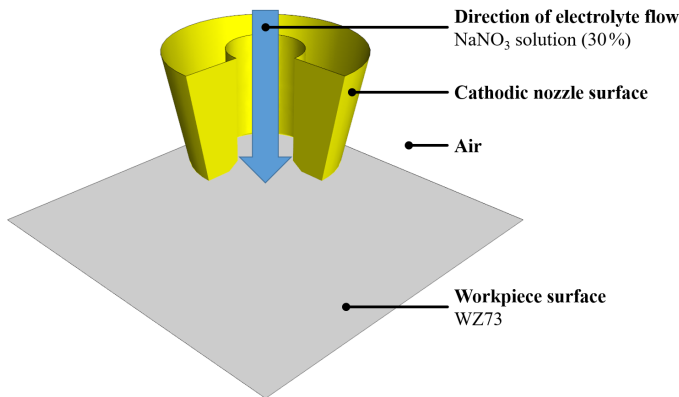


FIGURE 10 Simulation model of the Jet-ECM process for generating micro calottes in the workpiece surface.

TABLE 5 Process and material parameters used in the model of the Jet-ECM process.

Parameter	Value
Working voltage U_q	56 V
Electrolyte inflow velocity v_{el}	20 m s^{-1}
Working distance s_0	$100 \mu\text{m}$
Process time t_{proc}	2.0 s
Electrolyte conductivity σ_{el}	160 mS cm^{-1}
Electrolyte mass density ρ_{el}	1222 kg m^{-3}
Electrolyte dynamic viscosity η_{el}	$1.61 \times 10^{-3} \text{ Pa s}$
Air conductivity σ_{air}	$8 \times 10^{-6} \text{ mS cm}^{-1}$
Air mass density ρ_{air}	1.19 kg m^{-3}
Air dynamic viscosity η_{air}	$1.82 \times 10^{-5} \text{ Pa s}$

The process model utilizes the volume of fluid method for modelling the multiphase flow. For each finite volume element, mass density, electrical conductivity and dynamic viscosity are calculated according to the ratio of its immiscible components electrolyte and air. Based on the composition of each volume element, Maxwell's equations are solved for calculating the electric field for the given working voltage. The resulting current density distribution is determined according to the generalized Ohm's law. After the normal component of the current density on the workpiece surface has been derived, the removal is modelled according to the experimentally determined material characteristics (figure 5) by deforming its boundary.

3.2.2 | Results

Selected results of the Jet-ECM process simulation are shown in figure 11. Starting from left, the deformation of the workpiece surface and resulting changes in electrolyte flow are shown. While the electrolyte flow stays adhered to the surface at the start of the process, it changes drastically at a removal depth $z = 63 \mu\text{m}$ ($t = 0.34 \text{ s}$), ultimately causing a secondary electrical contact between nozzle and workpiece. The images in the middle depict the current density distributions on the workpiece surface, which results in higher removal velocities towards the center of the machined area, generating the characteristic calotte shape. Its profile can be seen on the right-hand side along the current density distribution in the electrolyte jet. In order to verify the accuracy of the developed model, several micro calottes were manufactured in a WZ73 sample for increasing machining times up to 2.0 s using a laboratory scale setup. Removal depths obtained in simulations and experiments are compared in figure 12, showing an average deviation of 4 %.

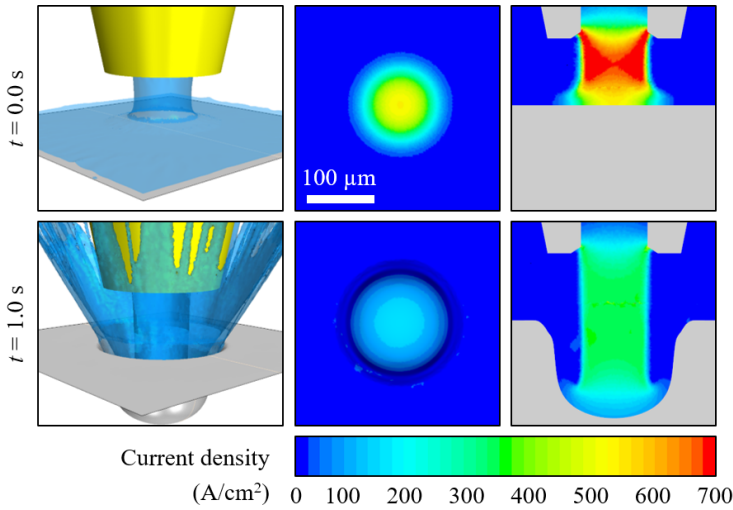


FIGURE 11 Manufacturing micro calottes in a WZ73 surface. Removal geometry and flow of electrolyte (left), current density distribution on the workpiece surface (middle) and in the electrolyte jet (right) at process times $t = 0.0 \text{ s}$ and $t = 1.0 \text{ s}$.

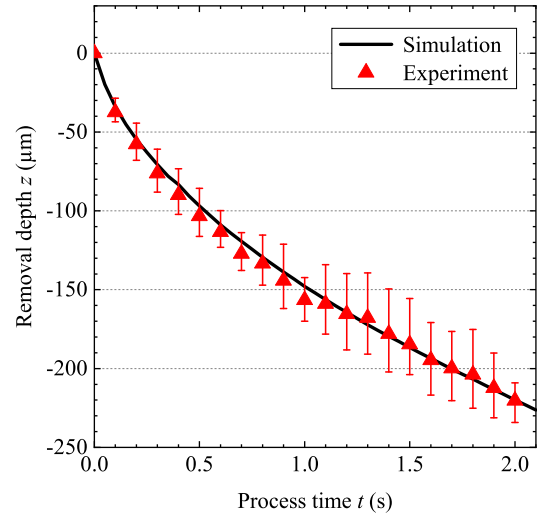


FIGURE 12 Comparison of removal depth z during the Jet-ECM process in simulation and experiment.

4 | SUMMARY AND CONCLUSION

In this work a methodology for designing ECM processes based on multiphysics simulation was presented. The data-driven approach utilizes a seamless flow of information on electrochemical material properties. It encompasses recording and processing process data as well as the development of interfaces between experiment, material database and process simulation model. The methodology was applied for two use cases in electrochemical micromachining: (i) the manufacturing of a centrifugal impeller with a diameter of 14 mm of the nickel-based superalloy Inconel 713C via pulsed electrochemical machining with oscillating cathode and (ii) the generation of micro calottes in the Mg-Y-Zn light metal alloy WZ73 via Jet-ECM. Characteristic material removal velocities and sums of overpotentials as functions of the normal current density were calculated and effective material removal rates derived. Based on requirements for the process simulation, suitable models using both FEM and FVM methods were developed. After integrating the material data into the models, transient process simulations were conducted. Having set suitable input parameters, current density distributions on the workpiece surface and resulting removal geometries were characterized. In addition, the reproduction accuracy of the cathode shape used in the PECM process was examined by evaluating lateral distances to the impeller blade. Micro calottes manufactured on a lab scale Jet-ECM setup were in good agreement with the simulation results regarding their relation between machining time and resulting depth, showing an average deviation of 4 %.

ACKNOWLEDGMENTS

The authors acknowledge the support of the project "Saxon Alliance for Material- and Resource-Efficient Technologies (AMARETO)" (Project No 100291455) that is funded by the European Union (European Regional Development Fund) and by the Free State of Saxony. Furthermore, they want to thank Prof. Dr. Rudolf Kawalla of Technische Universität Bergakademie Freiberg for providing sample material of WZ73.



Conflict of interest

The authors declare no potential conflict of interests.

References

1. Valenti M. Making the Cut. *Mechanical Engineering* 2001; 123(11): 64–67. doi: 10.1115/1.2001-NOV-4
2. Hackert-Oschätzchen M. Gestaltung von elektrochemischen Abtragprozessen durch Multiphysiksimulation gezeigt an der Endformgebung von Mikrobohrungen. In: Schubert A., ed. *Scripts Precision and Microproduction Engineering*. 10 of *Scripts Precision and Microproduction Engineering*. Verlag Wissenschaftliche Scripten. 2015.
3. INCO, The International Nickel Company, Inc. . Engineering Properties of Alloy 713C. Republished by The Nickel Institute; 1968. https://www.nickelinstitute.org/media/4686/ni_inco_337_engineering713.pdf. Accessed July 14, 2020.
4. Meichsner G, Hackert-Oschätzchen M, Zinecker M, Schubert A, Edelmann J. Pulsed Electrochemical Machining of Powder Metallurgy Steels. In: Mollay B, Lohrengel MM., eds. *Proceedings of the 7th International Symposium on ElectroChemical Machining Technology* 2011 (pp. 68–75). ISBN 978-3-00-036247-7.

5. Rajurkar K, Zhu D, McGeough J, Kozak J, De Silva A. New Developments in Electro-Chemical Machining. *CIRP Annals* 1999; 48(2): 567–579. doi: [https://doi.org/10.1016/S0007-8506\(07\)63235-1](https://doi.org/10.1016/S0007-8506(07)63235-1)
6. Watanabe H, Mukai T, Kamado S, Kojima Y, Higashi K. Mechanical Properties of Mg-Y-Zn Alloy Processed by Equal-Channel-Angular Extrusion. *MATERIALS TRANSACTIONS* 2003; 44(4): 463–467. doi: 10.2320/matertrans.44.463
7. Hackert-Oschätzchen M, Meichsner G, Zinecker M, Martin A, Schubert A. Micro machining with continuous electrolytic free jet. *Precision Engineering* 2012; 36(4): 612–619. doi: <https://doi.org/10.1016/j.precisioneng.2012.05.003>
8. Klocke F, Zeis M, Harst S, Klink A, Veselovac D, Baumgärtner M. Modeling and Simulation of the Electrochemical Machining (ECM) Material Removal Process for the Manufacture of Aero Engine Components. *Procedia CIRP* 2013; 8: 265–270. doi: <https://doi.org/10.1016/j.procir.2013.06.100>
9. König W, Klocke F. *Fertigungsverfahren 3: Abtragen, Generieren und Lasermaterialbearbeitung*. Springer Verlag. 4 ed. 2007. ISBN 978-3-540-48954-2.
10. Deutsches Institut für Normung e.V. . DIN SPEC 91399: Methode zur Bestimmung von Prozesseingangsgrößen für das elektrochemische Präzisionsabtragen – Anforderungen, Kriterien, Festlegungen. doi: <https://dx.doi.org/10.31030/3007935>; 2018
11. Loebel S, Hackert-Oschätzchen M, Meichsner G, Schubert A. Development of interfaces for material data integration in models of electrochemical machining processes. In: Michaelis A, Schneider M., eds. *International Symposium on ElectroChemical Machining Technology INSECT 2017 – Proceedings*. 6. Fraunhofer Verlag. 2017 (pp. 8–15). ISBN 978-3-8396-1261-3.
12. Loebel S, Hackert-Oschätzchen M, Meichsner G, Petzold T, Zinecker M, Schubert A. Modelling of Precise Electrochemical Machining for Nickel-based Centrifugal Impellers. In: Bähre D, Ernst A., eds. *Proceedings of the 15th International Symposium on ElectroChemical Machining Technology 2019* 2019 (pp. 193–202). ISBN 978-3-00-064086-5.
13. Loebel S, Hackert-Oschätzchen M, Meichsner G, Zinecker M, Schubert A. Simulation-based Design of Electrochemical Machining Processes for Microstructuring of High-strength Materials. In: Bergs T, Herrig T, Harst S, Klink A., eds. *Proceedings of the 14th International Symposium on ElectroChemical Machining Technology 2018* 2018 (pp. 145–156). ISBN 978-3-86359-667-5.

How to cite this article: Loebel S, Zinecker M Steinert P, and Schubert A (202X), Transient simulation of electrochemical machining processes for manufacturing of micro structures in high-strength materials, *Engineering Reports*, 202X;XXXXXX.